

# Frequency selective reconfigurable microstrip antenna for cognitive radio applications

**Dilip S. Aldar**

Karmaveer Bhaurao Patil College of Engineering, Satara, Maharashtra, India

Corresponding author: Dilip S. Aldar (e-mail: dilip\_aldar@rediffmail.com).

**ABSTRACT** For the efficient utilization of the electromagnetic radio spectrum, a cognitive radio communication system is employed, which deals with the spectrum scarcity. An efficient antenna is essential for the appropriate selection of the available frequencies. This paper presents a frequency-reconfigurable antenna design and implementation for cognitive radio applications. A reconfigurable inverted U-shape microstrip patch antenna fed by a 50-ohm microstrip line is designed and implemented. The designed and implemented antenna can be used for switching frequencies between 3.25 GHz and 4.1 GHz by choosing a specific sub-band from the specified wideband. The frequency reconfiguration is achieved by using twelve PIN diode switches by placing them on the slotted ground plane of the antenna by varying the antenna's effective length. The PIN diodes are organized in such a way as to alter antenna bandwidth and shift the operating band. The switching of PIN diodes is controlled using the microcontroller to select the appropriate frequency. Changes in effective length impede the path of surface currents and change the current density of the conductive patch. The performance of the simulated and fabricated antennas is investigated using different parameters. A good agreement between simulated and experimental results shows that the antenna is a good candidate for cognitive radio applications.

**INDEX TERMS** Cognitive Radio (CR), Microcontroller, PIN diode, Reconfigurable Antenna, Wideband.

## I. INTRODUCTION

THE electromagnetic radio spectrum is a scarce natural resource, the use of which by transmitters and receivers is licensed by governments. It is essential to use this scarce resource efficiently and effectively. Cognitive radio (CR) is one of the prominent candidates for effective spectrum utilization. Cognitive radio, inclusive of software-defined radio, has been proposed to promote the efficient use of the spectrum by exploiting the existence of spectrum holes [1]. Spectrum utilization can be improved significantly by allowing a secondary user (who is not being serviced) to access a spectrum hole unoccupied by the primary user at the right location and the time in question. In cognitive radio, if one user stops using part of the spectrum, another user can use that portion of the spectrum by employing the mechanism of identifying the unused spectrum and allocating it to the willing users. However, because frequency re-configurability is performed in the cognitive radio transceiver, a single antenna with fixed frequency tuning is ineffective for cognitive radio applications. To enhance the efficiency of the cognitive radio, reconfigurable antennas are crucial in cognitive radio systems.

In a CR system, the transceiver has to select a wide frequency band, in which the secondary user must be tuned to the empty spectrum hole, requiring higher hardware complexity [2]. The hardware complexity can be optimized using the

reconfigurable antenna for the dynamic selection of the frequency spectrum. The re-configurability enables a reduction in the hardware complexity of the communication system. Reconfigurability can be achieved in different parts of the communications system, and the antenna is one of them. A reconfigurable antenna can switch between different frequency bands, which reduces hardware complexity and the system's cost because a single antenna can be used for different applications. Multiple switches with wide and narrow band configurations can be used for frequency reconfiguration [3]-[13]. In [3], frequency reconfiguration is achieved with varactor diodes by adjusting capacitance values in the range of 0.5-2.2pF to have a frequency band of 1.2-1.65 GHz.

In [4], a varactors-based frequency reconfigurable antenna with a circular radiating patch is presented. It is tuned from 1.62 to 1.17 GHz when the capacitance of the varactors is varied from 0.6 to 1.8 pF. In [5], a reconfigurable multiband antenna is discussed, where two designs are demonstrated. The antenna supports GSM, DCS, PCS, and UMTS in the first design. The second design can support GSM, DCS, PCS, UMTS, Bluetooth, and 2.4 GHz wireless LAN. In [6-7], the reconfigurable antenna is capable of frequency switching between different frequency bands using PIN diode switches. In [8-10], reconfiguration is done through switching from wideband to narrowband, especially in Vivaldi antennas. In [11], an optically pumped reconfigurable antenna system is investigated where reconfiguration is carried out by

integrating laser diodes. Some examples [12–14] achieve reconfiguration by inserting notches. The integrated ultra-wideband (UWB) frequency reconfigurable is presented in [16–17] for the low power and wide band of frequency; the frequency selectability between the different bands is carried out using MEMS switches in [16] and using PIN diodes in [17].

In this paper, the presented antenna is simulated and designed using HFSS and implemented with an FR4 sheet. To select the appropriate frequency in the C-Band from 3.25 to 4.1 GHz, the PIN diodes are used. The antenna is suitable for cognitive radio, multimode and multiband wireless communication, which may allow coexistence with 5G (3.3–4.4 GHz) or WiMAX (3.3–3.6 GHz) or LTE (3.4–3.6 GHz) [18–19].

## II. SYSTEM APPROACH

Cognitive radio acts on cognition capability and reconfigurability. Cognitive ability refers to the identification of the white space of the wide spectrum that is not used by primary users at specific times and locations. Reconfigurability means that the cognitive radio system can switch between different parameters, such as frequency, radiation pattern, or polarization. These parameters can be programmed dynamically and are supported by the system.

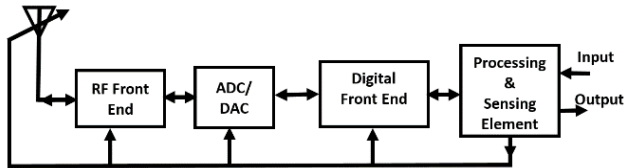


FIGURE 1. Cognitive radio front end

The major blocks in the cognitive radio transceiver are the transmitting/receiving antenna, RF front end, analog to digital converter (ADC), digital to analog converter (DAC), digital front end, sensing element, and processing section as illustrated in figure 1. The reconfigurable antenna reconfigures to the specific frequency band, which is a vacant space in the expected wide frequency band. The white spaces are sensed by the sensing element and sent to the antenna controller section in terms of the feedback signal. The antenna controller consists of the microcontroller and the microcontroller executes the algorithm and selects the appropriate configuration of the antenna where the specific frequency band is to be selected and allowed to the cognitive radio system.

## III. GEOMETRY, CONFIGURATION AND DESIGN

The antenna is implemented using an FR-4 epoxy substrate with a thickness of 1.6 mm, a dielectric constant ( $\epsilon_r$ ) of 4.4, and a loss tangent ( $\tan\delta$ ) of 0.020. The schematic of the presented antenna is shown in figure 2 in which figure 2 (a) shows its front view, which consists of a radiating element in the form of an inverted U, fed by a 50  $\Omega$  microstrip line. Figure 2 (b) shows its back view, which is slotted ground, consists of four slots into which twelve PIN diode switches are placed. The PIN diode BAR 50-03W from Infineon

Technologies was chosen because of the wide range of frequency of operation from 10 MHz to 6 GHz. The frequency reconfiguration is achieved by varying the length of the ground plane by adjusting the ON and OFF conditions of PIN diodes. The equivalent electrical model of the PIN diode is illustrated in figure 3 [20].

An electromagnetic (EM) solver, Ansoft HFSS, has been employed to simulate and analyze the electrical properties and radiation performance of the antenna. The parasitic inductance  $L = 1.8$  nH is used in both the OFF and ON states of the electrical model shown in figures 3(a) and 3(b).

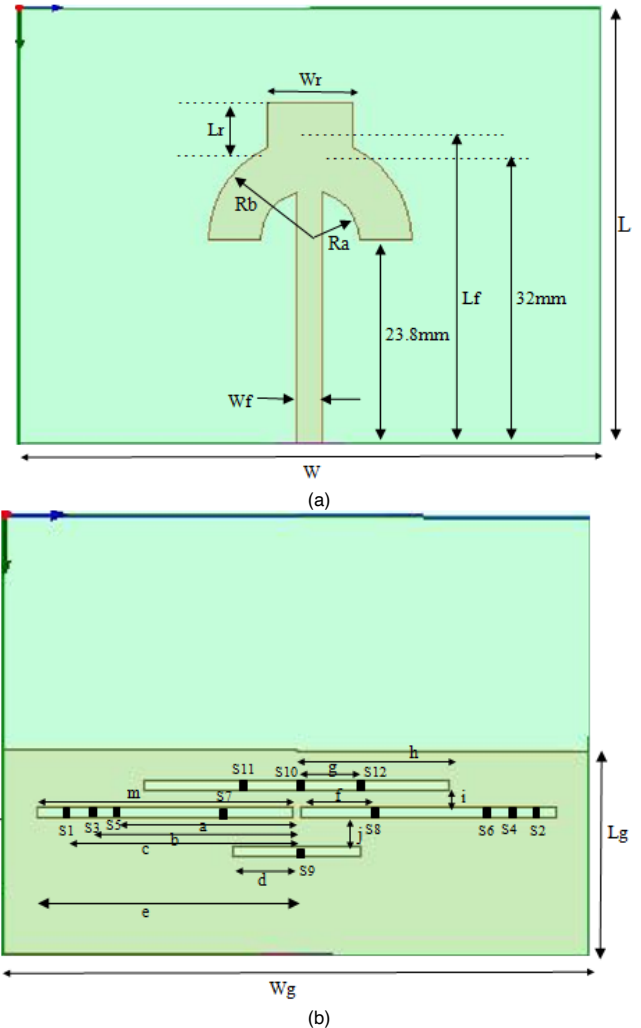
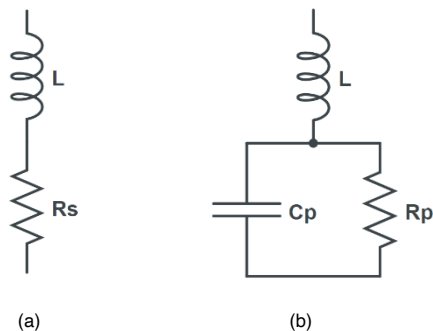


FIGURE 2. Schematic of proposed antenna: (a) front view; (b) back view.

For the OFF state (reverse biased), the circuit has a parallel combination of resistance and capacitance with  $R_p = 5$  k $\Omega$  and  $C_p = 0.15$  pF, and for the ON state (forward biased), only the resistance  $R_s = 3$   $\Omega$  is considered for simulation of the antenna.



**Figure 3.** RLC equivalent circuit model of PIN diode a) ON State, b) OFF state

The design dimensions have been optimized for the antenna to be matched over a particular frequency band, and the positions of PIN diodes are optimized on the crescents in order to obtain resonance frequencies close to the required standard frequency bands. The design parameters are summarized in Table I. The antenna switching combinations that correspond to the selected frequency configurations are illustrated in Table II.

**TABLE I.** Dimensions (mm) of the proposed design

Parameter	Value(mm)	Parameter	Value(mm)
a	23.6	g	5.6
b	25.6	h	17.7
c	27.6	j	3.3
d	7.5	Wf	3
e	30	Lf	30
f	8.6	Wr	10
i	1.8	Lr	8
Ra	39.75	Rb	45.90
Wg	68	Lg	22.52
W	68	L	51

**TABLE II.** Details of switch configuration

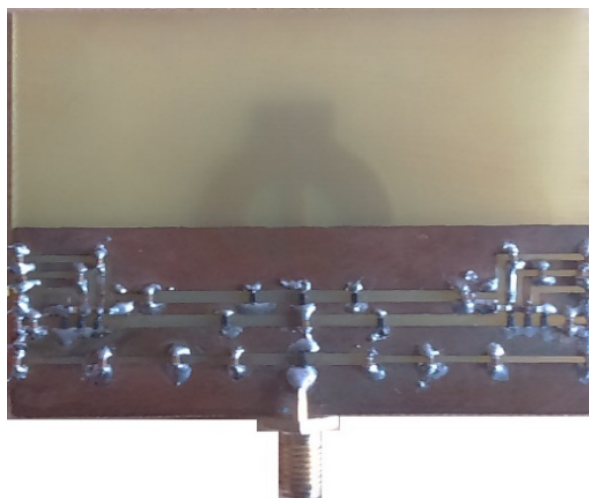
Configuration	Whole	Sub 1	Sub 2	Sub 3	Sub 4
S1	OFF	OFF	ON	OFF	OFF
S2	OFF	OFF	ON	OFF	OFF
S3	OFF	OFF	OFF	ON	OFF
S4	OFF	OFF	OFF	ON	OFF
S5	OFF	OFF	OFF	OFF	ON
S6	OFF	OFF	OFF	OFF	ON
S7	ON	OFF	OFF	OFF	OFF
S8	ON	OFF	OFF	OFF	OFF
S9	ON	OFF	OFF	OFF	OFF
S10	ON	OFF	OFF	OFF	OFF
S11	ON	OFF	OFF	OFF	OFF
S12	ON	OFF	OFF	OFF	OFF

### A. Antenna Fabrications

The antenna has been fabricated with FR-4 sheets and PIN diodes are used for varying the electrical characteristics of the antenna to achieve the reconfigurability as shown in Figure 4.



(a)



(b)

**FIGURE 4.** Fabricated Frequency reconfigurable antenna (a) Front view (b) Back view

Reconfiguration must be carried out by changing the length of the ground plane by making PIN diodes ON/OFF; 0.4 mm wide slots are introduced to separate ports of switches. To maintain DC separation and to provide RF continuity in the ground plane, 100 pF surface mount RF capacitors are used. These capacitors act as a short circuit for higher operating frequencies.

The fabricated antenna size is 68x51mm. As shown in Table II, to operate an antenna in a specific frequency band, the appropriate set of switching conditions should be chosen. The proposed antenna can be operated in wideband or any one of its four bands, with PIN diodes (S1– S12) used in the ground plane. To operate the antenna in any of the sub-band switches integrated into the middle slots (S1–S6), they are in the ON state in pairs to control the electrical length of the ground plane, and to operate the antenna in wideband mode, switches (S7–S12) are used to eliminate the effect of four

slots. The corresponding diode switching configuration is listed in Table II, to vary the effective electrical characteristics.

#### IV. RESULTS AND DISCUSSION

The presented reconfigurable antenna is simulated in HFSS and implemented on an FR-4 sheet. Both the simulated and experimented results are discussed in this section.

##### A. Reflection Coefficient

The reflection coefficient measures impedance discontinuity in the transmission medium. Figure 5 shows the simulated reflection coefficient, i.e., the return loss of different configurations. As it can be seen from Figure 5, by turning the different switches ON and OFF according to the configurations described in Table II, the antenna can be operated over the whole considered band or in one of four sub-bands with good in-band impedance matching. These results are achieved by matching one port with a  $50\Omega$  loaded microstrip line and exciting the other one.

In the range of 3.29-4.1 GHz, the reflection coefficient is more than -10 dB but still less than -7 dB, and that is acceptable as a fairly good performance in practical mobile communication. The return loss degrades as the resistance is increased. Multiple dips in the reflection coefficient curve are indications of closely distributed resonances as observed in the configurations.

##### B. Radiation pattern

The antenna radiation pattern is a mathematical function or a graphical representation of the radiation properties of the antenna as a function of space coordinates [15]. In most cases, the radiation pattern is determined in the far-field region and is represented as a function of the directional coordinates. Figure 6 shows a simulated 2-dimensional radiation pattern of a frequency reconfigurable antenna. The radiation pattern in the E-plane is a monopole butterfly-looking shape, and the H-plane is dipole-like. The patterns for the four sub-bands are almost identical, which is expected because the excited and radiated modes are the same.

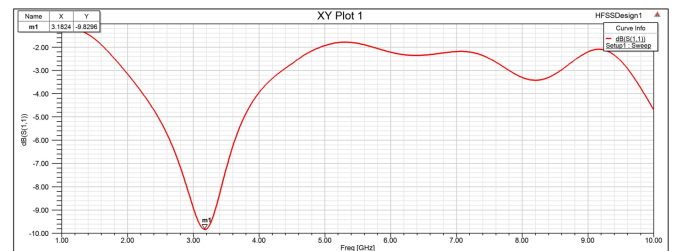
##### C. VSWR

The Voltage Standing Wave Ratio (VSWR) plot for an inverted U-shaped antenna is shown in Figure 7. Figure 7 (a) shows the VSWR of the whole band, which is 1.95. Figure 7 (b) shows the VSWR at 3.29 GHz is 1.92. Figure 7 (c) shows the VSWR at 3.50 GHz, which is 1.36. Figure 7 (d) shows the VSWR at 3.75 GHz, which is 1.27. Figure 7 (e) shows the VSWR at 4.1 GHz is 1.65, which indicates good impedance matching.

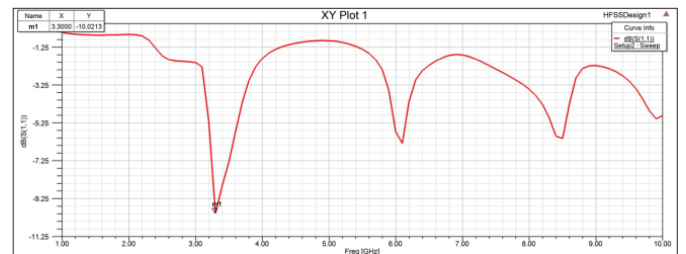
##### D. Current Distribution

The radiation properties of the antenna can be altered by variations in the current distribution along with the antenna. The effect of the  $50\Omega$  SMA feeding ports should not be ignored since they are very close to the antenna and their

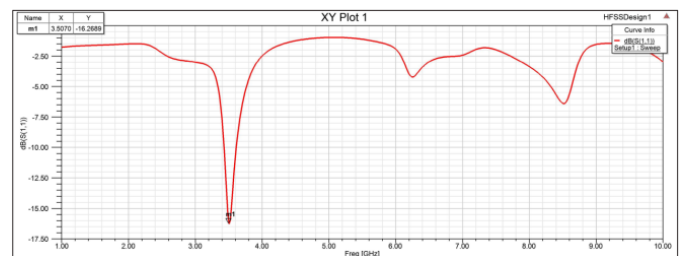
presence can change the current distribution on the antenna ground plane. To explore the EM behavior of the antenna, the current distributions on the antenna at different frequencies are shown in Figure 8. Currents are more concentrated on the edge of the radiator and in slots in the ground plane. The strong current distributions on the ground plane support the argument that the ground plane contributes to the impedance matching of this structure. The antenna radiates in traveling-wave mode, and the slot region close to the feeding gap supports travelling waves. Therefore, the narrowband antenna, which is further away, does not disturb the wideband patterns and the current distribution stays symmetrical.



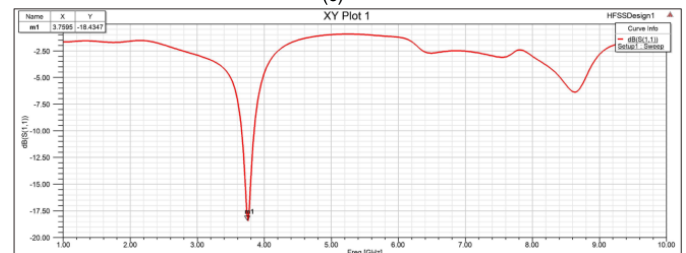
(a)



(b)

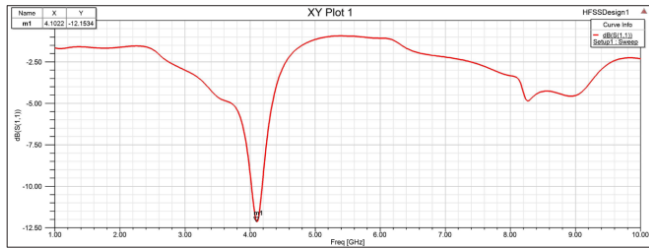


(c)



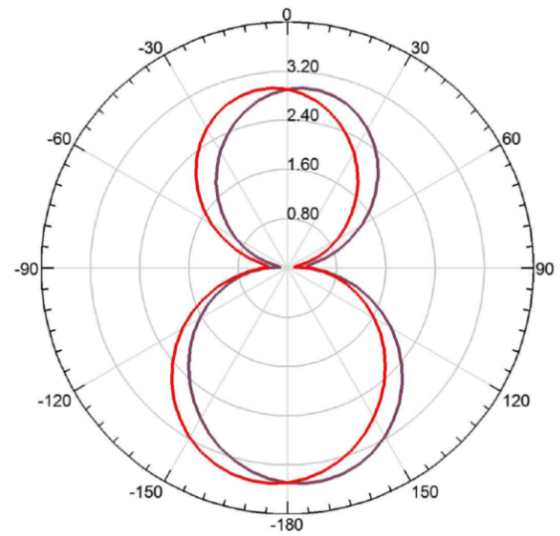
(d)



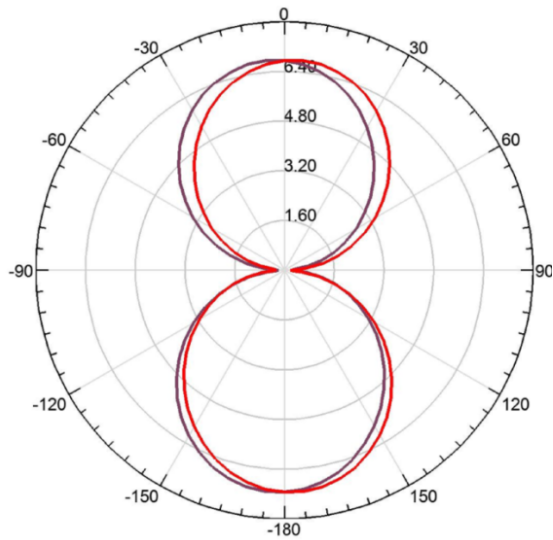


(e)

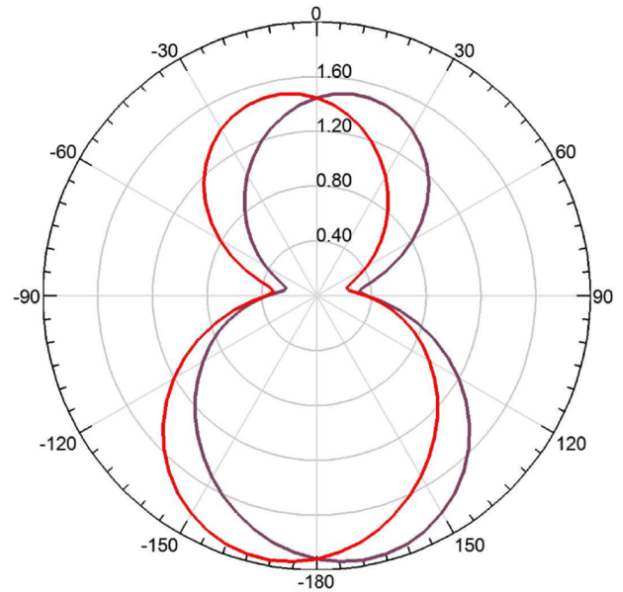
**FIGURE 5.** Reflection coefficient of (a) Whole band (b) Sub-band1 (c) Sub-band2 (d) Sub-band3 (e) Sub-band4



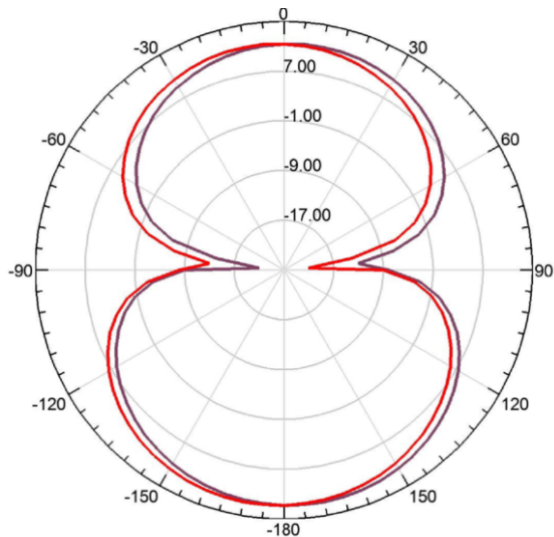
(c)



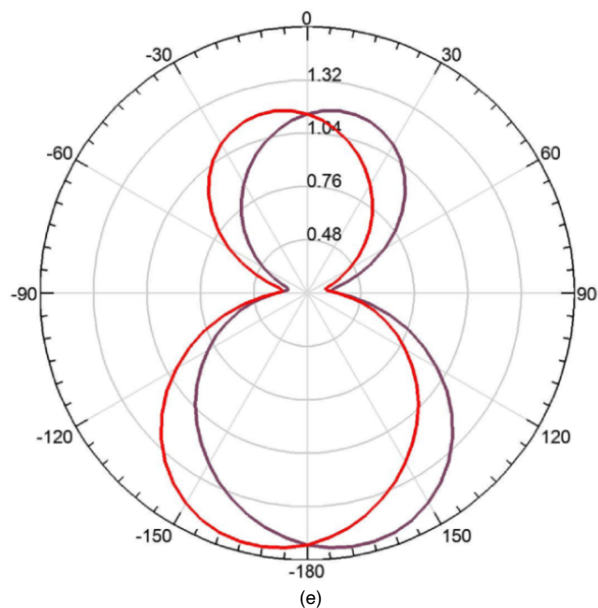
(a)



(d)

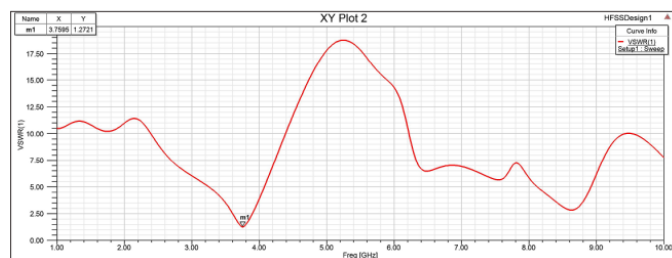


(b)

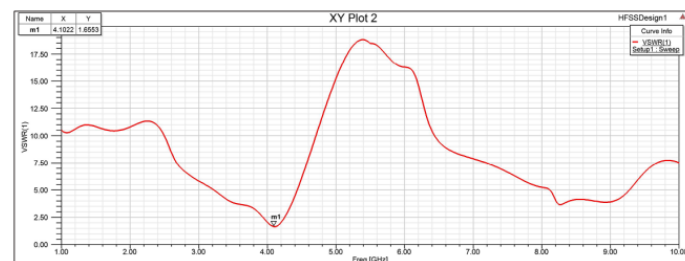


—  $\Phi=0^\circ$   
—  $\Phi=180^\circ$

**FIGURE 6.** Radiation pattern of (a) Whole band (b) Sub-band1 excited at 3.29 GHz (c) Sub-band2 excited at 3.50 GHz (d) Sub-band3 excited at 3.75GHz (e) Sub-band4 excited at 4.1GHz

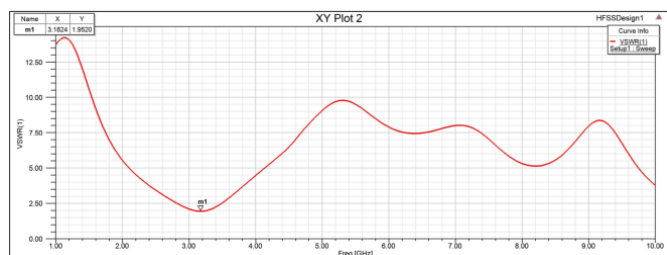


(d)

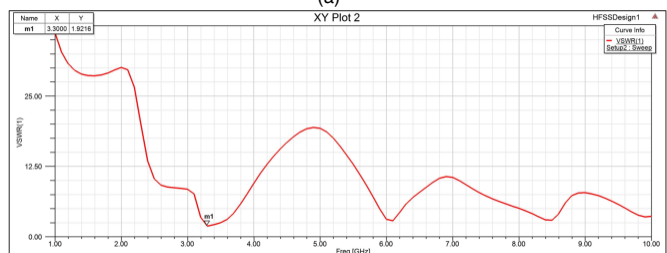


(e)

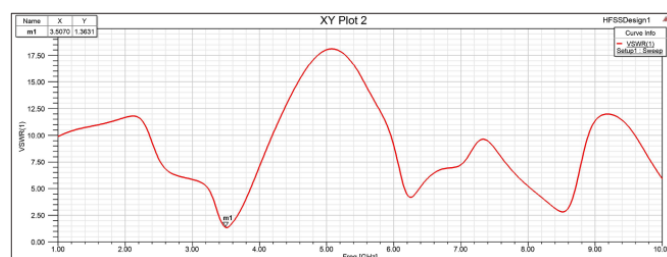
**FIGURE 7.** VSWR of (a) Whole band (b) Sub-band1 excited at 3.29 GHz (c) Sub-band2 excited at 3.50 GHz (d) Sub-band3 excited at 3.75GHz (e) Sub-band4 excited at 4.1GHz



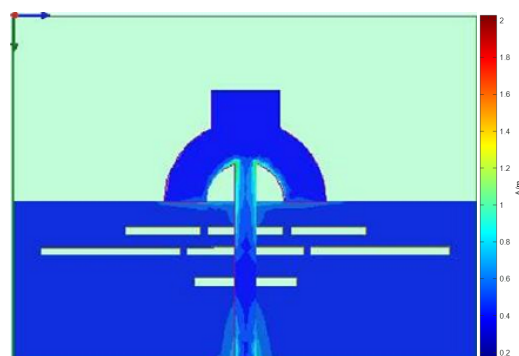
(a)



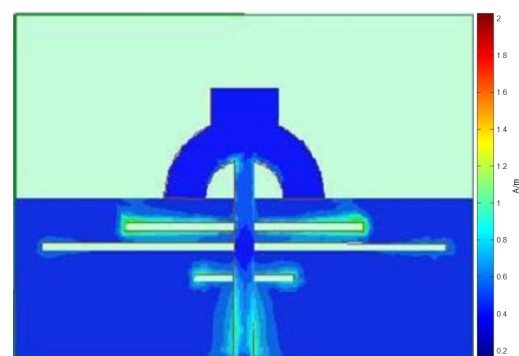
(b)



(c)



(a)



(b)

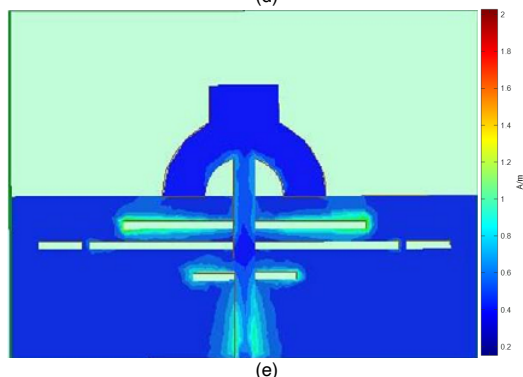
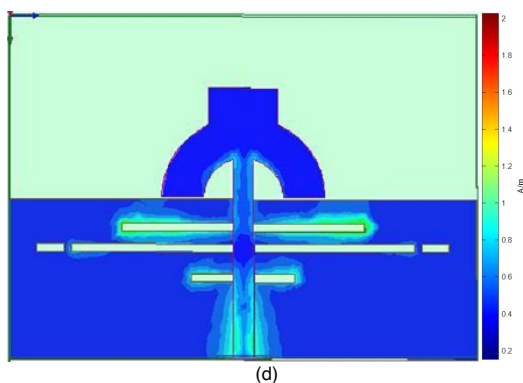
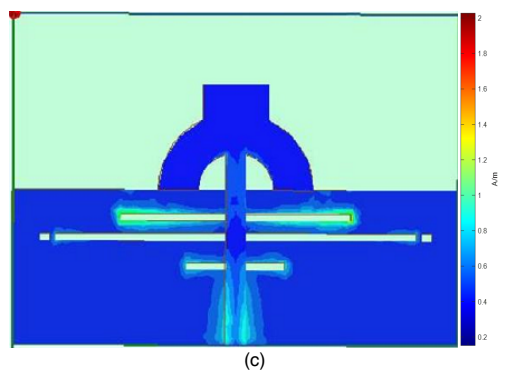


**FIGURE 8.** Surface current distribution of (a) Whole band (b) Sub-band1 excited at 3.29GHz (c) Sub-band2 excited at 3.50GHz (d) Sub-band3 excited at 3.75GHz (e) Sub-band4 excited at 4.1GHz

### E. Experimental Results

To validate the simulated result experimentally, the antenna is fabricated and tested in the laboratory environment. SMA connectors were soldered on the feed lines of the antenna to feed the signal and test the antenna by connecting it to a vector network analyzer. The Rohde & Schwarz vector network analyzer, whose frequency range is 300 kHz to 8 GHz, was used for testing the antenna. Figure 9 shows the photograph of the assembly of a fabricated antenna with the Arduino Mega board, which is used to control the antenna configurations. The switching among the respective sub-bands depends on the parasitic capacitance of the PIN diodes. The ON and OFF (i.e., forward and reverse bias) of the PIN diodes are controlled through the microcontroller. For testing purposes of the antenna, the microcontroller is programmed to switch the PIN diodes at specific intervals. A high

parasitic capacitance undesirably shifts the operational band towards the lower frequency range. This has prohibited the use of standard PIN diodes, for which the parasitic capacitances are usually ten times larger than the required value. As shown in Figure 10, a fabricated antenna is connected to the vector network analyzer for the measurement of the reflection coefficient.

Figure 11 shows the measured reflection coefficient of a reconfigurable antenna, which proves that the antenna can work either in wideband mode or in one of the sub-bands. Some frequency shifts are observed between simulated and measured results because the parasitic capacitance in the OFF state of the PIN diodes provided by the reconfiguration is smaller than that in the real ones. One of the important reasons why there are differences in the measured and simulated results is due to the approximate boundary conditions in the computational domain.

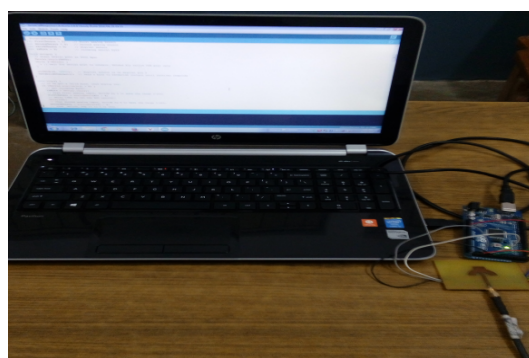


**FIGURE 9.** Fabricated antenna switching controlled by the microcontroller

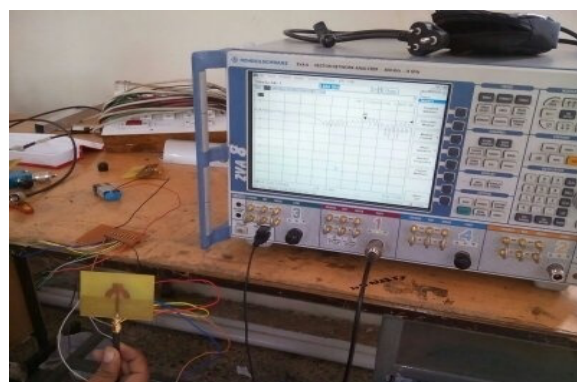


**FIGURE 10.** Fabricated antenna connected to Vector Network Analyzer

Moreover, the RF cable from the vector network analyzer slightly affects the measurements of small antennas. However, the main reason for that relatively poor rejection in S11 mainly comes from the dielectric losses of the FR4 substrate. A small frequency shift between the measurement and simulation is presumably due to the effect of parasitic in the PIN diodes, fabrication tolerances, and biasing components.

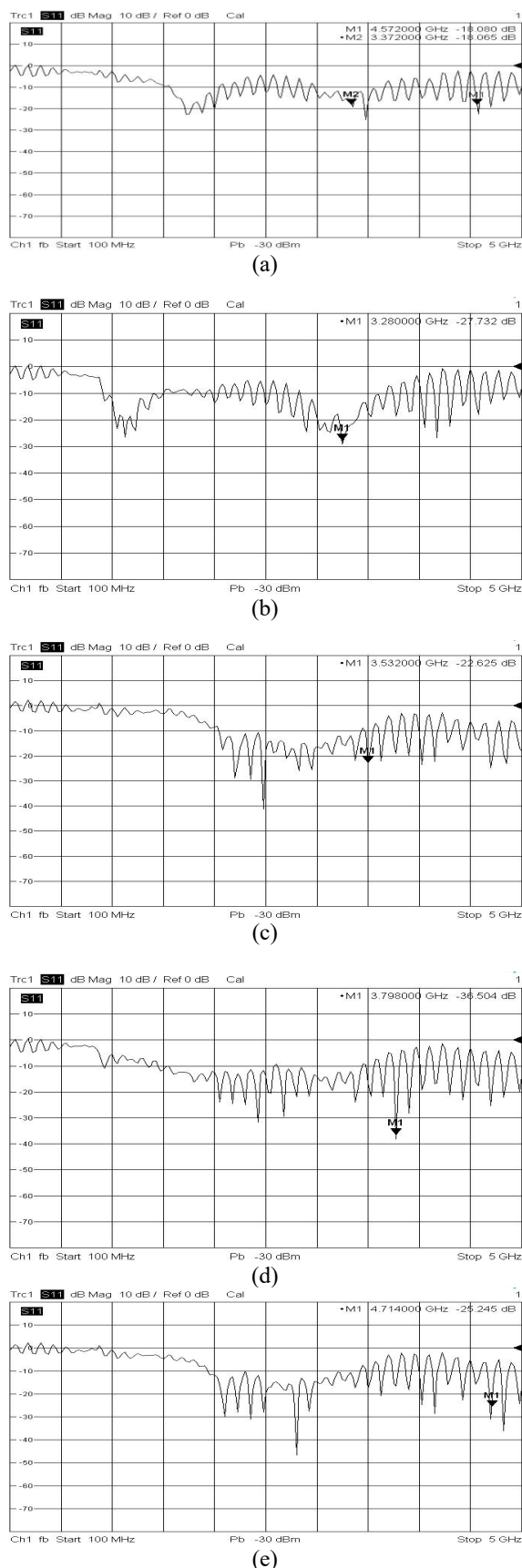


**FIGURE 11.** Measured Reflection Coefficient of (a) Whole band (b) Sub-band1 (c) Sub-band2 (d) Sub-band3 (e) Sub-band4

## V. CONCLUSION

The frequency reconfigurable antenna for cognitive radio applications of compact size using PIN diodes is designed to tune the tune over the different frequency bands by switching the PIN diodes. The simulated and fabricated antenna operates effectively in wideband and any of the sub-bands by changing the length of the ground plane and is composed of a monopole with a reconfigurable integrated filter in the ground plane. Both simulated and measured results have been presented, and a good agreement could be observed. The presented antenna has been offered with effective reconfigurability; therefore, the antenna could be a promising candidate for cognitive radio applications, including multimode and multiband communication applications.

## REFERENCES

- [1] S. Haykin, "Cognitive radio: Brain empowered wireless communications," *IEEE J. Se . Areas Commun .*, vol. 23, no. 2, pp. 201–220, Feb.2005.
- [2] P. S. Hall, Z. Hu, P. Song, M. R. Hamid, and Z. Wang, "Creating reconfigurable adaptive antennas for cognitive radio applications considering cost and portability," *IET Cognitive Radio Communications* 2010, London, U.K., 2010 .
- [3] N. Behdad and K. Sarabandi, "A varactor-tuned dual-band slot antenna," *Antennas and Propagation, IEEE Transactions on*, vol. 54, pp. 401–408, 2006.
- [4] Ting-Yan Liu, Jun-Yan Chen, and Jeen-Sheen Row, "Frequency Reconfigurable Antenna with Dual-Band and Dual-Mode Operation," *Progress In Electromagnetics Research Letters*, Vol. 97, 115–120, 2021. doi:10.2528/PIERL21031203
- [5] Angus C. K. Mak, Corbett R. Rowell, Ross D. Murch, and Chi-Lun Mak, "Reconfigurable Multiband Antenna Designs for Wireless Communication Devices," *IEEE Transactions On Antennas And Propagation*, Vol. 55, No. 7, July 2007.
- [6] Hassan Mirzaei, George V. Eleftheriades, "A Compact Frequency-Reconfigurable Metamaterial-Inspired Antenna", *IEEE Antennas And Wireless Propagation Letters*, Vol. 10, 2011.
- [7] A. Mansoul, F. Ghanem, Mohamad Rijal Hamid, Mohamed Trabelsi, "A Selective Frequency-Reconfigurable Antenna for Cognitive Radio Applications", *IEEE Antenna and Wireless Propagation Lett.*, vol. 13, 2014.
- [8] M. R. Hamid, Peter Gardner, Peter S. Hall, F. Ghanem, "Vivaldi Antenna With Integrated Switchable Band Pass Resonator", *IEEE Transactions On Antennas And Propagation*, Vol. 59, No. 11, November 2011.
- [9] M. R. Hamid, Peter Gardner, Peter S. Hall, F. Ghanem, "Switchable Band Vivaldi Antenna", *IEEE Transactions On Antennas And Propagation*, Vol. 59, No. 5, May 2011.
- [10] D. Dahalan, S. K. A. Rahim, M. R. Hamid, M. A. Rahman, M. Z. M. Nor, M. S. A. Rani, and P. S. Hall, "Frequency-Reconfigurable Archimedean Spiral Antenna", *IEEE Antennas And Wireless Propagation Letters*, Vol. 12, 2013
- [11] Youssef Tawk, Joseph Costantine, Sameer Hemmady, Ganesh Balakrishnan, Keith Avery, Christos G. Christodoulou, "Demonstration of a Cognitive Radio Front End Using an Optically Pumped Reconfigurable Antenna System (OPRAS)", *IEEE*



- Transactions On Antennas And Propagation, Vol. 60, No. 2, February 2012
- [12] Kenny Seungwoo Ryu, Ahmed A. Kishk, "UWB Antenna With Single or Dual Band-Notches for Lower WLAN Band and Upper WLAN Band", IEEE Transactions On Antennas And Propagation, Vol. 57, No. 12, December 2009.
  - [13] Parisa Lotfi, Mohammadnaghi Azarmanesh, Saber Soltani, "Rotatable Dual Band-Notched UWB/Triple-Band WLAN Reconfigurable Antenna", IEEE Antennas And Wireless Propagation Letters, Vol. 12, 2013.
  - [14] Nasrin Tasouji, Javad Nourinia, Changiz Ghobadi, and Farzad Tofigh, "A Novel Printed UWB Slot Antenna With Reconfigurable Band-Notch Characteristics", IEEE Antennas And Wireless Propagation Letters, Vol. 12, 2013.
  - [15] A. Balanis, Antenna Theory: Analysis and Design, 3rd ed.: A John Wiley and Sons Inc Publication 2005.
  - [16] Ros Marie C. Cleetus and Gnanadhas Josemin Bala, "Wide-Narrow Switchable Bands Microstrip Antenna for Cognitive Radios," Progress In Electromagnetics Research C, Vol. 98, 225-238, 2020. doi:10.2528/PIERC19102808.
  - [17] Ponnada Mayuri, Nagumalli Deepika Rani, Nemani Bala Subrahmanyam, and Boddapati Taraka Madhav, "Design and Analysis of a Compact Reconfigurable Dual Band Notched UWB Antenna", Progress In Electromagnetics Research C, Vol. 98, 141-153, 2020. doi:10.2528/PIERC19082903.
  - [18] The WRC series 3.5 GHz in the 5G Era preparing for new services in 3.3-4.2 GHz , October 2021, available at: <https://www.gsma.com/spectrum/wp-content/uploads/2021/10/3.5-GHz-for-5G.pdf>, accessed, July 2022
  - [19] 5G - C-Band Spectrum for 5G – October 2019, available at: <https://gsacom.com/paper/c-band-spectrum-for-5g-october-2019/>, accessed, July 2022.
  - [20] Datasheet for Infineon BAR 50-03W, silicon PIN diode, Infineon Technologies AG, available at: <http://www.farnell.com/datasheets/1500311.pdf>, accessed, July 2022.